J Mater Sci: Mater Electron (2021) 32:2590–2600

Novel technique for large area n-type black silicon solar cell by formation of silicon nanograss after diffusion process

Soma Ray[1,2], Suchismita Mitra[3], Hemanta Ghosh[3], Anup Mondal[2,4], Chandan Banerjee[5,*], and Utpal Gangopadhyay[1]

[1] Centre of Advanced Research in Renewable Energy and Sensor Technology, MSIT, Kolkata 700150, India
[2] Centre of Excellence for Green Energy and Sensor Systems, IIEST, Shibpur, Howrah 711103, India
[3] National Centre for Photovoltaic Research and Education, IIT Bombay, Mumbai, India
[4] Departments of Chemistry, IIEST, Shibpur, Howrah 711103, West Bengal, India
[5] National Institute of Solar Energy, Gwal Pahari, Gurugram 122003, Haryana, India

Received: 11 July 2020
Accepted: 1 December 2020
Published online:
2 January 2021

© The Author(s), under exclusive licence to Springer Science+Business Media, LLC part of Springer Nature 2021

ABSTRACT

Metal-assisted chemical etching (MACE) method is the most convenient and cost-effective nanowire fabrication method compared to other nanowire fabrication processes although a major problem arises in silicon nanowire, formed by MACE solution during n-type c-Si solar cell fabrication steps. High-temperature boron diffusion in conventional open tube furnace breaks down the nanowire resulting in a non-uniform surface pattern which is responsible to decrease overall conversion efficiency of the finished cell. In this work, this drawback is resolved by considering silicon nanowire formation after diffusion step. A slow etchant is considered for nanostructure on diffused silicon wafer to protect the diffused junction. The generated nanowire size is very less and has forage-like structure, and so termed as nanograss. Surface morphology and the characterization of the silicon nanograss structure after diffusion process on large area (156 mm × 156 mm) c-Si solar cells using MACE method have been investigated elaborately. Further, the complete solar cell has been fabricated with an efficiency of 17.20%.

1 Introduction

Solar cell technology has been enormously spread out throughout the world due to recent emphasis on renewable energy resources. Global PV market has expanded by 25% in the year 2019 reaching up to 129GW solar installations [1]. Silicon Solar cells dominate the overall growing solar cell market due to high efficiency and durability. The efficiency of solar cells is predominated by optical and electrical loss [2]. To reduce optical loss, different anti-reflective coating is used although using the coating solar cell

Address correspondence to E-mail: utpal_ganguly@yahoo.com

https://doi.org/10.1007/s10854-020-05027-6

processing charges are augmented [3]. So minimization of reflection along with cost-effective technique is the ultimatum. It has already been reported that silicon nanowires (Si NW) is a highly demanding technology due to its broadband absorption of optical spectrum [4]. There are lots of techniques which have been already adopted worldwide to fabricate SiNW solar cells like reactive ion etching (RIE), electrochemical etching, vapor liquid solid (VLS), metal-assisted chemical etching (MACE) etc. [5]. MACE is the most convenient and cost-effective method to fabricate vertically aligned SiNW arrays [6]. The shape and size of the nanowire can easily be adjusted with the change in chemical proportions of MACE solution [6]. Despite these advantages of the MACE process, a difficulty has arisen. Silicon nanowire substrate by MACE process is not appropriate for conventional n-type solar cell diffusion step by open tube furnace. N-type solar cell emitter surface is structured by boron diffusion in conventional open tube furnace which is a high-temperature ($\sim$ 950–1000 °C) prolonged process. The chamber ambience should be kept with proper balancing of nitrogen and oxygen. By the variation of process timing and temperature, different diffusion profiles can be obtained. At this high-temperature ambiance, silicon nanowire starts to crack and after boro silicate glass removal step all the nanowires are wiped out. This is due to highly porous nature of silicon nanowire by MACE [7].

Kaiwang Zhang et.al (2009) has reported that silicon nanowire melting point varies with its diameter and after 900 °C it starts to melt [8]. This is why n-type black silicon solar cells are usually made up of RTA diffusion which is not a conventional industrial process. Junyi Chen et al. (2017) used RTA (rapid thermal annealing) diffusion method in silicon nanowire by metal-assisted chemical etching and improved efficiency up to 8.7% after selective etching [9]. Ioannis Leontis et.al (2018) also reported diffusion method by spin coating of boron source followed by high-temperature treatment in n-type silicon nanowire solar cell [10]. Deepika Bora et al. (2019) has used phosphorous spin dopant solution to form p-type emitter in silicon nanowire solar cell. The diffusion temperature was carried out at 990 °C [11].

To validate it, in this paper, the industrially feasible black silicon solar cell process was adopted first. At first, the experiment was done in a different way and with different composition of MACE solution. Single steps as well as double step MACE process parameters have been varied, but after high-temperature treatment of boron-diffused emitter surface, all the nanowires have wiped out. Surface morphology and process parameters have been widely demonstrated. A novel method was adopted to overcome this difficulty and the process sequence has been changed a little. The target was fixed to fabricate nanowire after the diffusion process. So diffusion with low sheet resistance has been adopted first and then the nanowire was formed by single step and double step MACE process, but at this moment, the emitter junction of n-type c-Si silicon solar cell was worn off. Sheet resistance variations before and after the diffusion step were demonstrated here. This happened due to the high etch rate of HF in MACE solution. So, to slow down the etch rate, we have replaced HF with NH_4F and sheet resistance was monitored accordingly. In this condition, silicon nanograss structure has been formed on a textured silicon surface. Around 90-100Ω/□, sheet resistance was achieved after nanograss formation on boron-diffused emitter surfaces. After that, passivation and metallization were done accordingly for the betterment of solar cell performance.

2 Experimental details

2.1 Chemical etching

A series of experiments on bare and diffused silicon etching to grow nanostructure were carried out with different approaches. The silicon substrate used in this study was n-type c-Si (100) with resistivity (ρ = 2-5Ω-cm). The samples were first cleaned with acetone and isopropyl alcohol and then by piranha solution (3:1concentrated H_2SO_4/30% H_2O_2) for 10 min. Textured silicon surface has been formed by 2% KOH and 6.5% IPA and 0.15% NaOCl solution. The fabrications of SiNW were carried out by different methods. In the first part of the experiment, nanostructured silicon surface has been formed by single step MACE, $AgNO_3/HF/H_2O_2/HNO_3$ (0.01:4:1:2) for 2-10 min. The resultant silicon surface was copiously cleaned with deionized water. In the second part, SiNW was formed by double step MACE, $AgNO_3$/HF (0.008 M: 1.5 M: 100 ml H_2O) in 1st solution and HF/H_2O_2(1.5 M: 1.2 ml: 100 ml H_2O) in 2nd solution for 3-5mins. In both cases

uniform, SiNW arrays were grown on a textured silicon surface. Then the emitter diffusion step in a conventional open tube furnace was carried out with BBr_3 source kept at 20 °C. The pre-deposition temperature was 945 °C for 15 min, but, in both cases, the nanowire was wiped out totally after prolonged heat treatment in the diffusion step. In the third part of the experiment, Si NW was formed after the diffusion step with a single- as well as double step MACE process. The diffusion parameter was kept the same as before, but in that case, the diffusion junction was removed totally or a non-uniform diffused surface was formed after etching. Sheet resistance before and after the diffusion process was measured elaborately. In the fourth part of the experiment, we have changed the etching solution by replacing HF with NH4F as NH4F has a slower etched rate than HF. In this part diffused, silicon substrate was etched by 2 M NH_4F/0.008 M $AgNO_3$/2 ml H_2SO_4 (1st sol) and 2 M NH_4F/1.5 ml (30%) H_2O_2/2 ml H_2SO_4 (2nd sol). Sheet resistance reflectance and FESEM before and after the diffusion process have been measured.

2.2 Solar cell fabrication

In this work, conventional methods of solar cell fabrication have been used like BBr_3front and $POCl_3$ rear diffusion, plasma-enhanced chemical vapor deposition (PECVD) for silicon nitride (SiNx) deposition as antireflection coating (ARC), and screen-printed metallization for contact. The samples prepared in the first and second part of the experiment were diffused initially by BBr3 on the front side as the diffusivity of boron was low so a high temperature was needed for p-type diffusion. The diffusion was carried out at different pre-deposition temperatures like 925 °C, 935 °C, 945 °C, and 955 °C with a variation of time from 20-30 min. After diffusion, the surface of silicon changed to a gray color which indicates that the SiNWs were wiped out. To verify these FESEM images were investigated, now we have to adopt an alternating step where we have implemented a novel technique of SiNW Solar cell by replacing SiNW formation after the diffusion step. Front surface diffusion has been done first by BBr_3 source. Different diffusion profiles were taken with different sheet resistance. Pre-deposition and drive-in temperature and time were varied to obtain different sheet resistance diffusion profiles. The rear surface was diffused by $POCl_3$ source to obtain n + layer. Sheet resistance was measured after that. In this condition, single- and double step MACE solutions were used for fabrication nanowire after the diffusion step. The chemical compositions of single and double step MACE solutions were the first and second part of the experiment. After immersing the diffused wafers in a single step and double step MACE solution, the surface turned to non-uniform black. After measuring the sheet resistance, it was observed that the junction has been removed in some places or junction depth was very low. This happened due to the high etch rate of HF. To reduce the etch rate, an alternating solution was necessary. In this paper, we have selected NH_4F as a good replacement of HF to slow down the etch rate. Silicon nanograsses (SiNG) were grown on diffused silicon wafer by NH4F MACE solution, 2 M NH_4F/0.008M$AgNO_3$/2 ml H_2SO_4 (1st sol), and 2 M NH4F/1.5 ml(30%) H_2O_2 / 2 ml H_2SO_4 (2stsol) for 15 s in 1st solution and 2 min for 2nd solution. Reflection and sheet resistance were measured accordingly. As SiNG was formed after the diffusion process, there was no need for edge isolation because the edge was already etched during SiNG etching. The front surface was passivated by $Al_2O_3$by GEMSTAR T-ALD at temperature 175 °C. The thickness of the passivating layer was kept at 10 nm. In some samples about 80 nm, SiNx layer was deposited by standard PECVD technique as for barrier layer. The front and back metallization of the samples were carried out by using standard Ag–Al paste at front and Ag paste for back by screen printing followed by baking and firing at RTP furnace. Finally, the fabricated solar cells were tested using a Solar simulator under a standard condition of AM 1.5 Global spectrum with a temperature of 25 °C (Fig. 1).

3 Results and discussions

3.1 Formation of silicon nanowires (SiNW)

In the following section, we have investigated the structural, optical, and electrical properties of SiNW Solar cells. Our first attempt was fabrication of SiNW by (a) single step ($AgNO_3$/HF/H_2O_2/HNO_3 (0.01:4:1:2)) and (b) double step ($AgNO_3$/HF (0.008 M:1.5 M:100 ml H_2O) in1st solution and HF/ H_2O_2 (1.5 M: 1.2 ml: 100 ml H_2O) in 2nd solution) MACE process. FESEM study (Carl Zeiss Microscopy

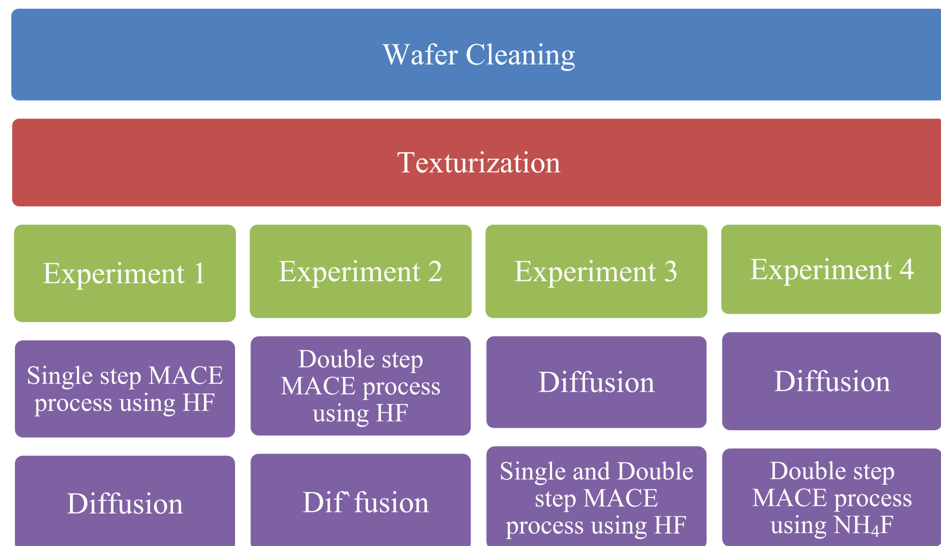

Fig. 1 Process flow adopted for the experiments

Ltd, Sigma 02–87) (Fig. 2a) of attempt (a) showed petal-like nanostructures on a textured silicon surface. At 10,000 KX magnifications we have seen, the nanowire was not formed properly, but a nanoporous structure was formed. To justify the optical property, we have taken a reflectance curve by UV–VIS-NIR spectrophotometer (Shimadzu, solid-spec 3600) for different solution concentrations and a different time. The best results obtained by changing different parameter concentrations and the time of the reaction are shown in Fig. 2b. Solar weighted Average Reflection (SWAR) reflection of single step Si NW was around 4%.

Now we have tried to move to the objective for formation of n-type crystalline Si NW by double step MACE (2 M NH_4F/0.008 M $AgNO_3$/2 ml H_2SO_4 (1st sol) and 2 M NH_4F/1.5 ml (30%) H_2O_2/2 ml H_2SO_4 (2st sol)). FESEM image in Fig. 3a shows thin nanowires grown on a textured silicon surface. Nanowires were magnified and the heights of the nanowire are 200–400 nm. Time and solution concentration were changed and few variations of reflectance are shown in Fig. 3b.

3.2 Formation of diffused junction

After the formation of Si NW successively on a textured Si surface, we have to move to diffusion in an open tube furnace. Boron diffusion has been performed at an elevated temperature > 900 °C to make boron silicon bonding. Different diffusion profiles were performed with different temperatures and pre-deposition time, but a difficulty arose rigorously after the diffusion process. It was seen that nanowires were wiping out after the diffusion process. Figure 4a shows a textured silicon n-type wafer. After the formation of Si NW, color has been changed to pitch black (Fig. 4b) due to multiple reflections. In Fig. 4c it is shown that after the diffusion process when the borosilicate glass was removed, the color was changed totally and turned into white. This indicated the removal of Si NW from the surface.

To validate the result, various diffusion profiles with varying sheet resistance were performed on both single and double step nanowire samples. After the diffusion process, nanowires were wiped out in the maximum region. Here, statistical data has been presented with the percentage of area covered by SiNW and the sheet resistance of the aforementioned area. Figure 5a and b indicated the statistical data of single and double step nanowire conditions after the diffusion process. We have taken 25 variations of diffusion profile and so different sheet resistances have been found accordingly, but in most of the cases, Si NW by single step existed within 2–35% of the total area of the silicon wafer after BSG removal of diffusion step. The bar chart has represented the area of the wafer where nanowire resides after the diffusion step and the spheres were corresponding to the sheet resistance of the wafer.

The percentage area of nanowire existence after double step diffusion was mostly 20–30%. Here nanowire stability after diffusion was higher than single step nanowire formation. This was because the

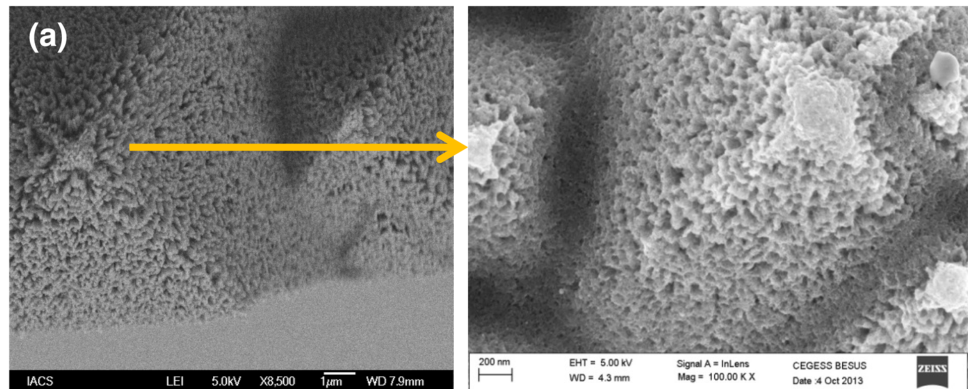

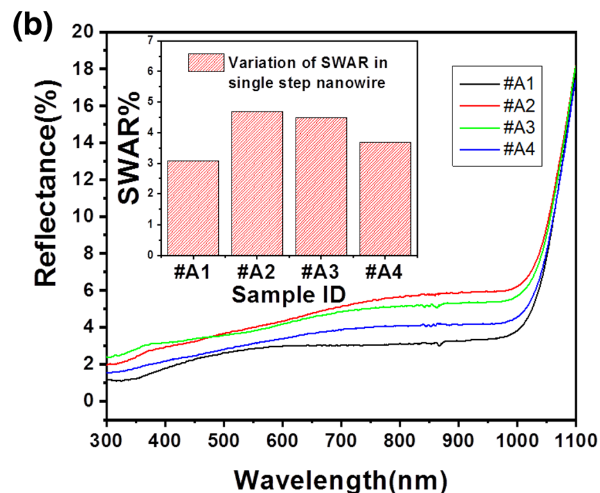

Fig. 2 **a** FESEM image with different magnification and **b** Reflectance of single step SiNW

pore formation probability was low compared to the process for single step nanowire formation. The wiping out of the nanowire from the wafer surface after the diffusion process occurred because the MACE process not only formed the nanowires, but also nanopores. In the high-temperature diffusion step, after prolonged heat treatment, the nanoporous structures have turned into microporous structures. So, when borosilicate glass (BSG) was removed in HF treatment, the nanowires from the substrate were wiped out, so solar cell performance was degraded. In this situation, it was decided to fabricate Si NW after a diffusion process. Figure 6 indicated the non-uniformity of Si NW growth after diffusion step.

3.3 Fabrication of SiNW after diffusion process using HF

In this case, high junction depth with low sheet resistance was required because the process of nanowire etching resulted in reduction of the junction depth followed by enhancement of sheet resistance. In commercial solar cells, a sheet resistance of 90–100Ω/□ is maintained. So, it was our prime target to achieve sheet resistance within the aforementioned range after nanowire etching. In primary condition, emitter diffusion was done on a textured silicon surface. Different diffusion profiles were used. Pre-deposition temperature varied from 900–97 °C. After borosilicate glass (BSG) removal by 5% HF solution, phosphorous doping was done at 900 °C with sheet resistance 20-22Ω/□ at the rear side. After diffusion, followed by phosphosilicate (PSG) glass removal, Si NW was formed by single and double step MACE process. Time of etching varied from 20–50 s. After nanowire formation, type test was necessary for p-type emitter surface on n-type silicon wafer by hot probe test method. In profile 1, 2, and 3, 5 junctions were there, but implied V_{oc} was very small and sheet resistance was 300-600Ω/□ which were not adequate for a highly efficient solar cell. Moreover, the growth of the nanowire was also non-uniform. In profiles 4 and 6 of

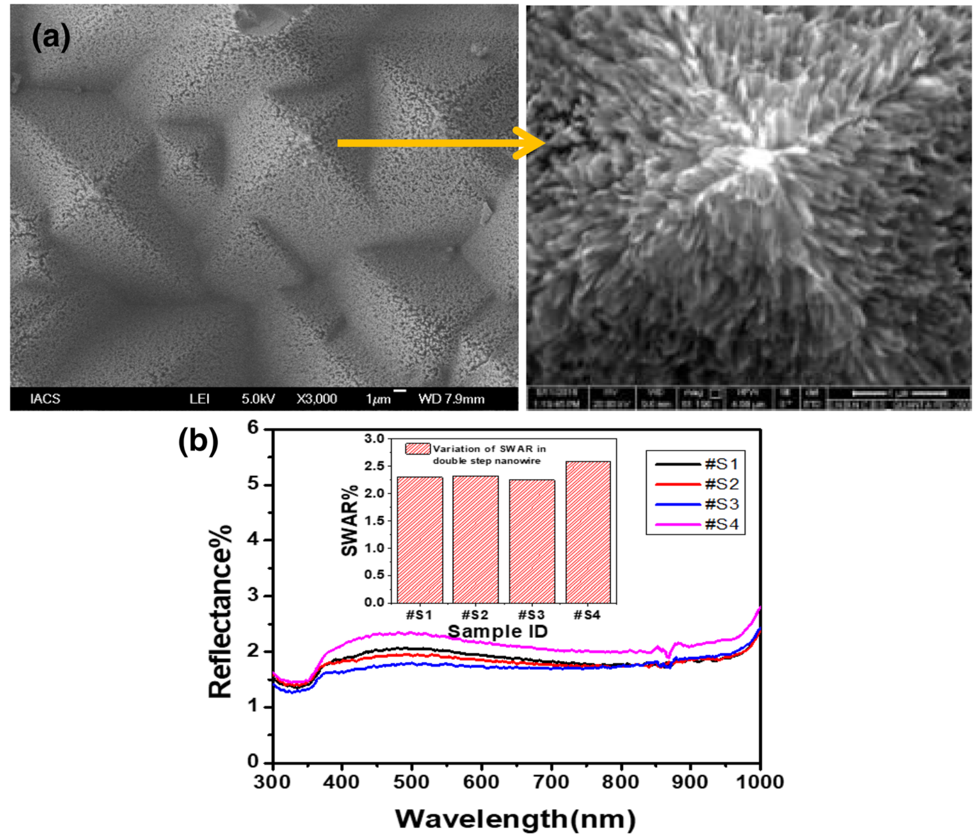

Fig. 3 **a** FESEM image of Si NW on Textured Si wafer and **b** Reflectance of double step Si NW

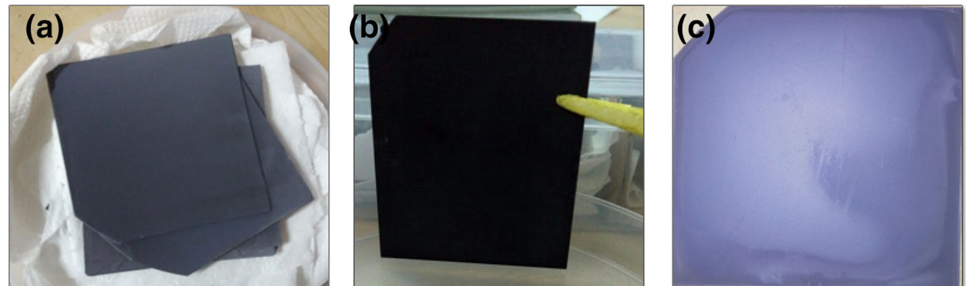

Fig. 4 Image of **a** Textured, **b** nanowire on textured, and **c** diffusion on textured nanowire surface

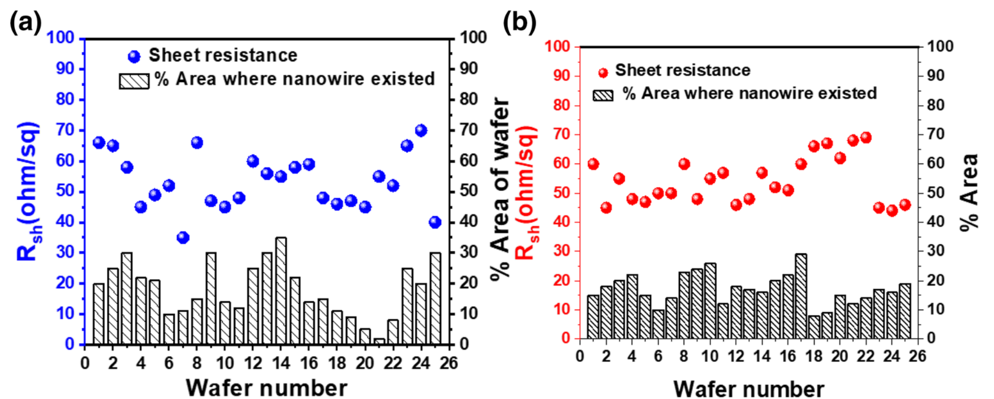

Fig. 5 Variation of R_{sh} and the percentage of area where nanowire by **a** single step **b** double step MACE process is present after diffusion for 25 different wafers

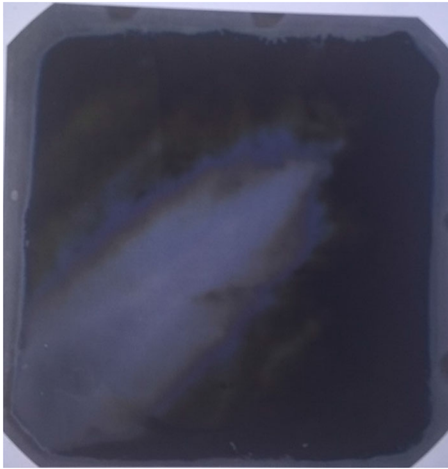

Fig. 6 Indication of the non-uniformity of Si NW growth after diffusion step

Table 1, semiconductor junction has been removed totally after the formation of Si NW in both single and double step MACE. So, the implied V_{oc} measured by SINTON WCT-120 showed 0.1 V.

This situation happened due to the high etch rate of HF which is used in both single and double step MACE solutions. So, we have to choose a slow etchant to slow down the etch rate and to control Si NW formation process.

3.4 Fabrication of SiNW after diffusion process using NH_4F

Following the failure of the formation of SiNW after the diffusion process using etching methods with HF, we adopt a new method by replacing HF with ammonium fluoride (NH4F). This was a unique solution for nanograss formation as the etching rate was lower than HF and this process was environment friendly also. In our previous work, we have characterized the etching solution [6]. We have calculated the etch rate for each process. Etching of wafers by HF and NH4F was done followed by weight measurement. The weight reduction was observed after specific time duration as shown in Fig. 7. It became evident from Fig. 7 that NH4Fwas etching at a slower rate compared to HF.

In this method, the solution was made up of $AgNO_3 + NH_4F + H_2SO_4$ in the ratio of 2 M NH_4F + 0.008 M $AgNO_3$ + 2 ml H_2SO_4(1st sol) and 2 M NH_4F + 1.5 ml (30%) H_2O_2 + 2 ml H_2SO_4 (2nd sol) in aqueous solution and FESEM and reflectance graph are shown in Fig. 8a and b, respectively. Height of the textured surface was 4-5um. Then conventional emitter diffusion was done by BBr_3 source with different pre-deposition temperature. The sheet resistance (Rsh) was varied accordingly. Table 2 elaborated the method.

Si NG arrays were grown all over the diffused textured surface. The height of the nanograss was 200-300 nm range giving an impression of grass and hence named as silicon nanograss. It can be observed that silicon nanograss was grown uniformly all over the samples. Both 78 mm × 78 mm and 156 mm × 156 mm samples were used for the experiment and the same results were observed.

After formation of nanograss on textured diffused silicon sheet, resistance increased upto 90–100 Ω/□ (in Table 2) which was quite good for betterment of solar cell performance.

AFM image was also observed to study the surface morphology. Figure 9a shows the AFM image where the textured surface and the rough surface on the textured surface due to the formation of nanograss are clearly visible. To study optical absorption of silicon nanograss after the diffusion step, the reflectance was measured by UV–VIS-NIR spectrophotometer as shown in Fig. 9b. With decreasing time of etching from 1.5 min to 1 min in batch #S3 sample P2

Table 1 Variation of sheet resistance and implied V_{oc} with different diffusion profiles after chemical etching for NW formation

Profile no	Diffusion profile(pre Dep temp in °C)	No. of MACE steps	Etching time (sec)	Sheet resistance (R_{sh} = ohm/sq)	Implied V_{oc} (mV)
1	900	Double	20	302–398	380
2	955		25	358–485	320
3	930		30	560–610	240
4	945		50	55	0.1
5	970	Single	20	490–570	315
6	940		30	49–52	0.1

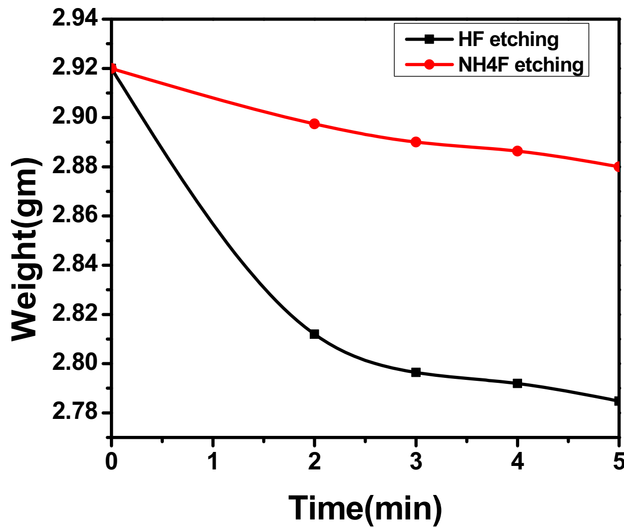

Fig. 7 Etch rate of HF and NH_4F for nanowire and nanograss structure

showed lower reflectance compared to #P1. SWAR for #P2 reduced to 1.6% which was much better than nanograss structure by MACE solution.

Silicon nanograss lattice fringes were clearly seen in Fig. 9c. The lattice spacing is of the order of 2.4 Å that clearly matches with the standard spacing value of silicon. The selected area diffraction pattern (SAD) has been taken at different portions of the sample and they mostly remain the same. TEM data cannot claim that it is single crystalline along nanograss, but they have a good degree of crystallinity with crystallographic grain size [13]. EDAX data confirms that the sample contained the majority element silicon along with a little bit of oxygen.

3.5 Surface passivation using dielectric layer of Aluminum Oxide (Al_2O_3)

A 10-nm-thick aluminum oxide (Al2O3) has been deposited on the front surface of the samples with nanograss by standard T-ALD, Gemstar instrument for surface passivation. In this case, Trimethylaluminum precursor (TMA) from Sigma-Aldrich kept at room temperature and de-ionized water were used as source material for Al_2O_3 layer deposition. The total deposition process was done in an inert N_2 atmosphere at 10sccm flow rate. The process temperature was 175 °C. We have used 84 cycle deposition to grow up 10-nm-thick Al_2O_3 film. We have measured the minority carrier lifetime and implied V_{oc} of the as-deposited Al_2O_3 and the lifetime data of textured, textured diffused nanograss, and Al_2O_3 on nanograss-diffused textured n-type c-Si as been shown in Fig. 10. Maximum implied V_{oc} was measured to 0.590 V. It has been predicted after the firing step of

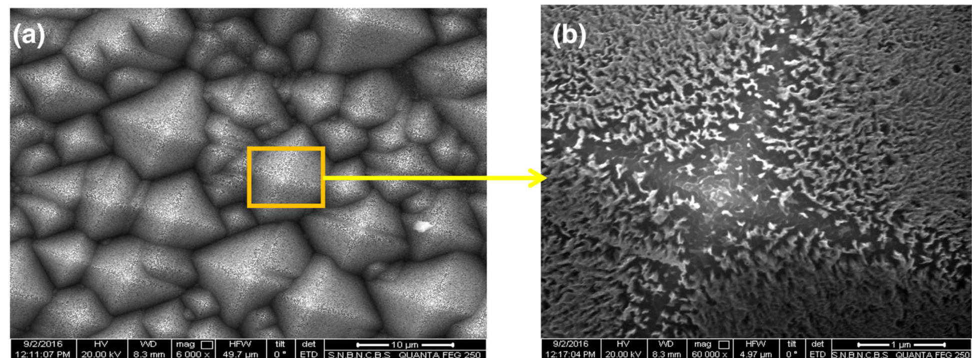

Fig. 8 FESEM of Si NW by NH_4Fdouble step MACE process with **a** magnification 10,000 × and **b** magnification 80000x

Table 2 Variation of sheet resistance with different diffusion profiles after chemical etching of SiNG formation

Sample number	Diffusion parameter	R_{sh}(Ω/□) before SING formation	R_{sh}(Ω/□) after SING formation
#S1	925 °C (Pre dep temp) for 20 min	20–22	80–90
#S2	945 °C (Pre dep temp) for 10 min	25–28	82–90
#S3	955 °C (Pre dep temp) for 15 min	45–47	95–100
#S4	920 °C (Pre dep temp) for 17 min	30–33	85–98
#S5	935 °C (Pre dep temp) for 15 min	35–40	83–92

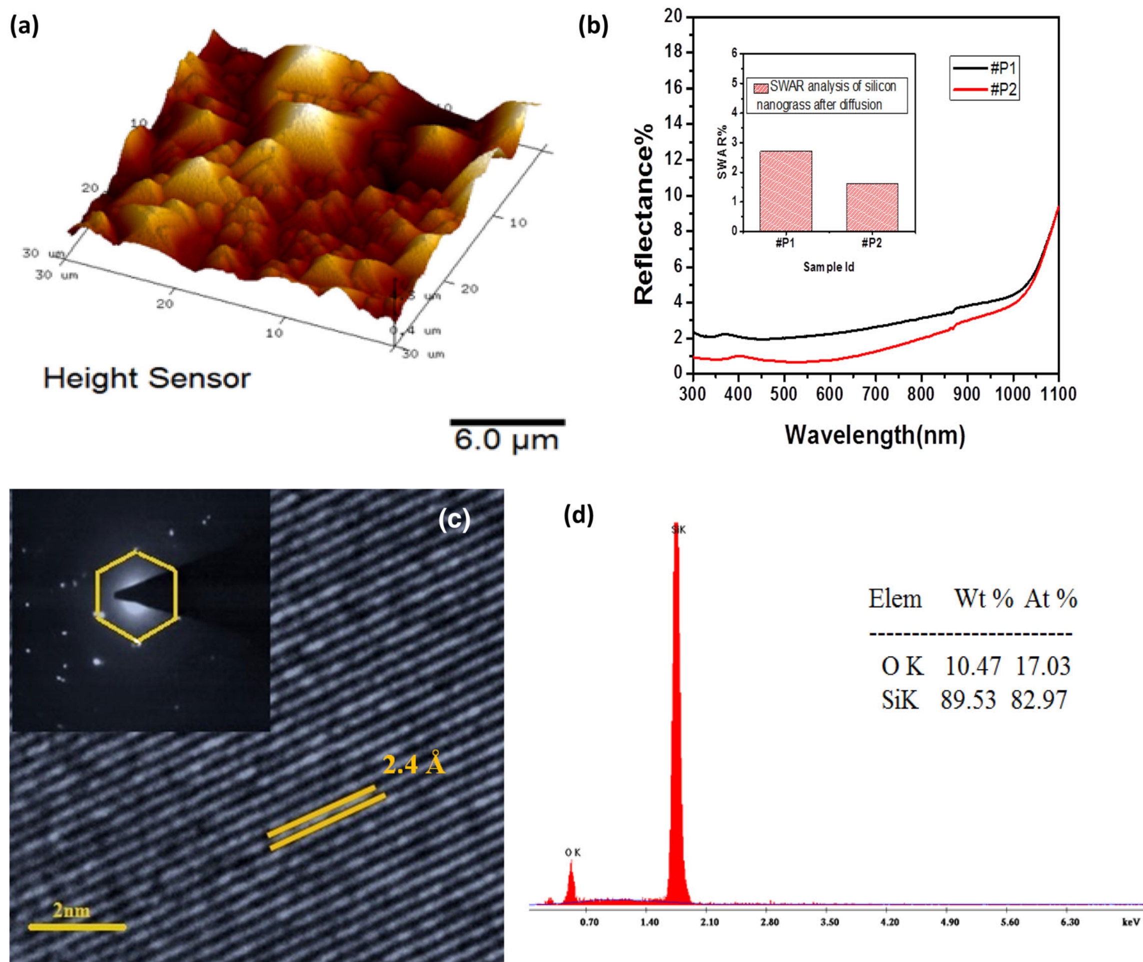

Fig. 9 **a** AFM of textured nanograss silicon **b** Reflectance of silicon nanograss by NH_4F double step MACE process after diffusion **c** TEM image of silicon nanograss(inset SAED pattern of silicon nanograss) **d** EDAX of silicon nanograss structure

the finished solar cell Voc would be increased [14, 15].

Some nanograss samples were coated with SiNx to make a barrier layer and avoid damaging Si NWs during firing. This further improved the passivation of the wafers. Reflectance was measured on SiNW after textured diffused silicon, Al_2O_3 on SiNW textured diffused silicon, and SiNx on Al_2O_3 of SiNW textured diffused silicon surface as shown in Fig. 11. After SiNx deposition, the optical property of the wafer has been degraded.

After deposition of SiN_x/Al_2O_3 of Si nanograss on the diffused silicon wafer, metallization was carried out with standard Ag–Al paste at front and Ag paste for back by screen printing followed by drying and firing in an RTP furnace. Best result was obtained for Al_2O_3-coated nanograss samples. Figure 12 showed the I-V characteristic curve under 1 sun (measured by PET Photoemission Tech. Inc.) and Suns-Voc curve (measured by SINTON) for the best large area black silicon solar cell that was fabricated. The champion cell exhibited 17.20% efficiency with J_{sc} = 36.81 mA/cm^2 and V_{oc} = 607 mV under 1sun illumination, while Suns-Voc result showed 18.07% efficiency, although Jsc and Voc were the same (Table 3). The Suns-V_{oc} curve showed the I-V characteristics of the solar cell in the absence of series resistance (R_s). A presence of series resistance R_s = 1.35Ω.cm^2 resulted in loss of fill factor (FF). This indicated that better optimization of firing techniques during the process of metallization may further increase with lower series resistance and higher fill factor. Additionally, better front and rear surface passivation can also improve efficiency.

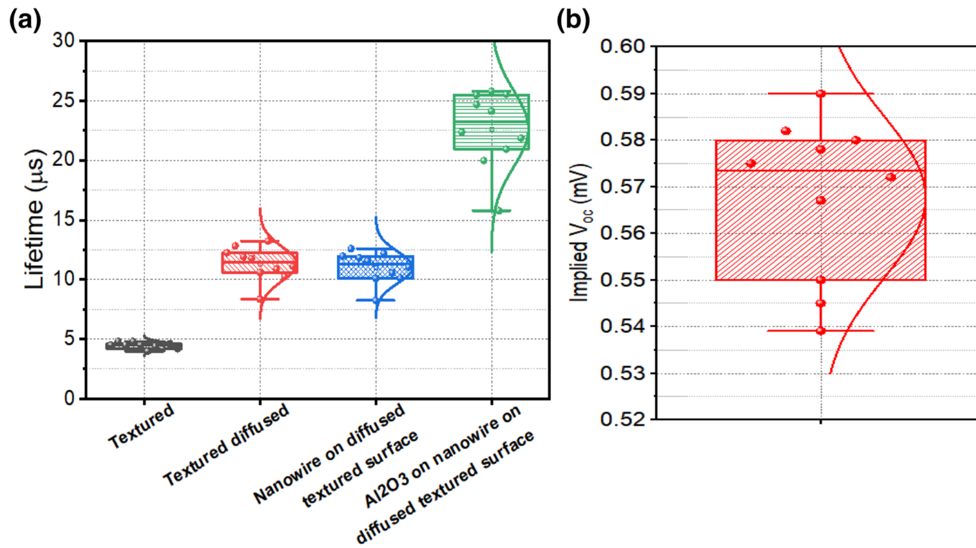

Fig. 10 Statistical distribution of lifetime and implied Voc for different samples

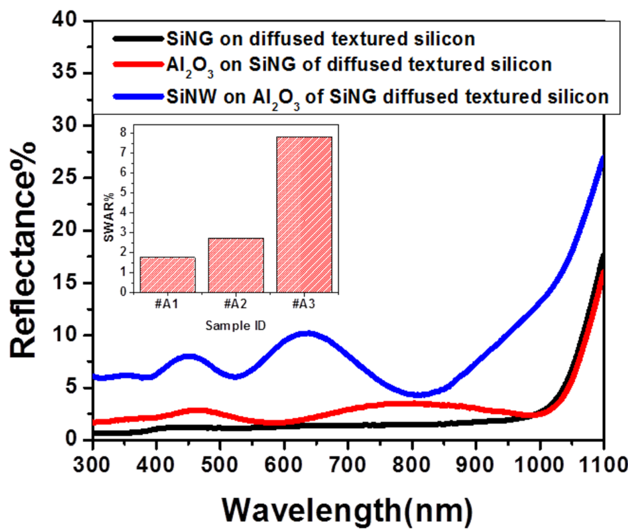

Fig. 11 Reflectance of textured diffused silicon with Si nanograss, Al_2O_3 on Si nanograss, and SiNx/ Al_2O_3 on Si nanograss on top

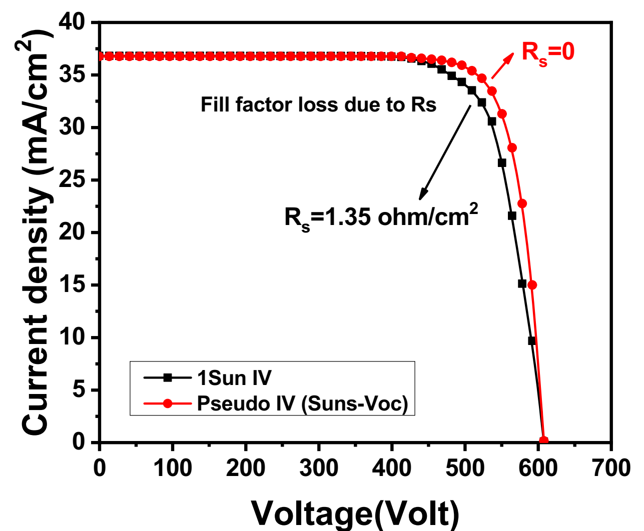

Fig. 12 Comparison of I-V characteristics curve of the champion solar cell using Si nanograss technique

4 Conclusion

The application of Silicon nanowires (SiNW) by Single or Double Metal Assistant Chemical Etching (MACE) has been attempted in the Solar cell process sequence due to its low cost and low reflectance properties compared to the costly Silicon Nitride (SiNx) conventional ARC process. But a basic problem for the incorporation of this SiNW ARC process in the industrial process sequence is its elimination in the solar cell process sequence chain. The long time high-temperature diffusion cycle of SiNW on a textured silicon wafer in an open tube furnace was no longer maintaining SiNW structure. This was probably due to the formation of porous structures formed during the MACE process. So it is a significant constraint to fabricate a solar cell by conventional process sequence chain of solar cell. Even after changing the process sequence chain by forming SiNW after diffusion, a high etching rate of MACE solution using HF results in non-uniform distribution of nanowires on the surface along with the removal of diffusion junction. In this paper, a novel approach was adopted by introducing the black silicon/nanograss formation step after the diffusion

Table 3 Solar cell parameters of champion cell

J_{sc} (mA/cm^2)	V_{oc} (mV)	FF (%)	Efficiency (%)	Rs (Ω.cm^2)	Rsh (Ω.cm^2)	Pseudo Efficiency (%)
36.81	607	77	17.20	1.35	845.32	18.07

process, but changing chemical constituents in the MACE, by using NH_4F instead of HF. As a result, a well-defined nanograss structure was formed on a diffused silicon wafer. Incorporation of a low etching rate of NH_4F kept the diffused junction with optimum junction depth, which is an achievement of our paper. Further, passivation by Al_2O_3 using ALD was carried out to final cell fabrication of solar cells. After optimization, black silicon/nanograss solar cells were made by little modification of cell fabrication process sequence and finally an efficiency of 17.20% for the champion cell was achieved.

Acknowledgement

The authors are grateful to the SERI DST, Govt. of India for financial support to carry out solar cell-related research. The authors deeply acknowledge Meghnad Saha Institute of Technology, TIG for providing the infrastructural support to carry out this research. The authors are also thankful to CEGESS, IIEST for infrastructural support. The authors are deeply grateful to Mr. Arindam Ray (Research fellow at JNCASR) for language correction support.

References

1. https://www.smart-energy.com/renewable-energy/global-solar-pv-market-returns-to-double-digit-growth-in-2019.
2. Mauricio Arias,Mackarena Briceño, Aitor Marzo, Antonio Zárate, "Optical and electrical properties of silicon solar cells by wet chemical etching", J. Chil. Chem. Soc. vol.64, (2019).
3. Kumaragurubaran.B, Anandhi.S, "Reduction of reflection losses in solar cell using Anti Reflective coating", International Conference on Computation of Power, Energy, Information and Communication (ICCPEIC), (2014).
4. Md Ali Asgar, Mehedhi Hasan, Md Fazlul Huq & Zahid Hasan Mahmood, "Broadband optical absorption measurement of Si NWs for photovoltaic solar cell applications", International Nano Letters,vol.4,(2014).
5. V. Schmidt, J.V. Wittemann, S. Senz, Si NWs A Review on Aspects of their Growth and their Electrical Properties. Adv. Mater **21**, 2681–2702 (2009)
6. Soma Ray, Anup Mondal, Utpal Gangopadhyay, "Optimization and characterization of silicon nano-grass antireflection layer on textured silicon wafer", Applied Physics A, vol.126, (2020).
7. S. Ray, S. Ghosh, H. Ghosh, S. Mitra, C. Banerjee, A.K. Mondal, H. Saha, S. Jana, S. Das, B. Pal, U. Gangopadhyay, "Fabrication of Nanowire on micro Textured Crystalline Silicon Wafer Before and After Diffusion Process A comparative study of solar cell performance. Journal of Materials Today: Proceedings **4**, 1278–12683 (2017)
8. Liu Wen-Liangy, Zhang Kai-Wang, and Zhong Jian-Xin, "Thermal stability of silicon nanowires: atomistic simulation study", Chinese Physics B, 2920–05,(2009).
9. Junyi Chen, Thiyagu Subramani, Wipakorn Jevasuwan, Naoki Fukata (2017) Improvement of silicon nanowire solar cells made by metal catalyzed electroless etching and nano imprint lithography Japanese. Journal of Applied Physics, 56: 04CP03
10. I. Leontis, M.A. Botzakaki, S.N. Georga, A. Galiouna Nassiopoulou, Study of Si Nanowires Produced by Metal-Assisted Chemical Etching. ACS Omega **3**, 10898–10906 (2018)
11. D. Bora, S. Bhattacharya, N. Kumar, A.B. Mallick, A. Srivastava, M. Dutta, S.K. Srivastava, P. Prathap, C.M.S. Rauthan, Performance Limitation of Si Nanowire Solar Cells Effects of Nanowire Length and Surface Defects. AIP Conf. Proc. **2162**, 020115 (2019)
12. S. Ray, A. Mondal, U. Gangopadhyay, "Optimization and Characterization of Silicon Nano-grass Antireflection Layer on Textured Silicon Wafer. Journal of Applied Physics A **126**, 399 (2020)
13. Adel Najar and Amine El Moutaouakil, "Hybrid Silicon Nanowires for Solar Cell Applications", Doi: https://doi.org/10.5772/intechopen.742821
14. D. Pysch, J. Ziegler, J.-P. Becker, D. Suwito, S. Janz, S.W. Glunz, and M. Hermie,"Potentials and development of amorphous silicon carbide heterojunction solar cells", Photovoltaic Specialists Conference (PVSC), 34th IEEE, (2009).
15. S. Choi, K.H. Min, M.S. Jeong, J.I. Lee, M.G. Kang, H.-E. Song, Y. Kang, H.-S. Lee, D. Kim, K.-H. Kim, "Structural evolution of tunneling oxide passivating contact upon thermal annealing. Scientific Reports **7**, 12853 (2017)

Publisher's Note Springer Nature remains neutral with regard to jurisdictional claims in published maps and institutional affiliations.